ELSEVIER

Chemical Geology 193 (2003) 25–41

CHEMICAL GEOLOGY
INCLUDING
ISOTOPE GEOSCIENCE

www.elsevier.com/locate/chemgeo

REE diffusion in feldspar

D.J. Cherniak *

Department of Earth and Environmental Sciences, Rensselaer Polytechnic Institute, 110 8th Street, West Hall, Troy, NY 12180, USA

Received 26 March 2002; accepted 16 August 2002

Abstract

Diffusion of several rare-earth elements has been characterized in natural plagioclase under dry, 1-atm conditions. Polished or cleaved sections of feldspar were surrounded by source powders in Pt capsules and annealed in air. Sources of diffusant were rare-earth aluminate garnet powders produced by combustion synthesis. Prepared sample capsules were annealed for times ranging from 30 min to a few months, at temperatures from 925 to 1350 °C. The REE distributions in the feldspars were profiled by Rutherford Backscattering Spectrometry (RBS).

The following Arrhenius relation is obtained for Nd diffusion in oligoclase (An_{23}), for diffusion normal to (010):

$$D = 2.3 \times 10^{-3} \exp(-425 \text{ kJ mol}^{-1}/RT) \text{ m}^2 \text{ s}^{-1}.$$

Diffusion in normal to (001) appears to be slightly faster than diffusion normal to (010).

For anorthite (An_{93}), Nd diffusion normal to (010) corresponds to the Arrhenius relation:

$$D = 5.9 \times 10^{-6} \exp(-398 \text{ kJ mol}^{-1}/RT) \text{ m}^2 \text{ s}^{-1}.$$

Diffusion rates of four rare earths (La, Nd, Dy, Yb) were measured in labradorite (An_{67}). For transport normal to (010), the Arrhenius relations are:

$$D_{La} = 1.1 \times 10^{-2} \exp(-464 \text{ kJ mol}^{-1}/RT) \text{ m}^2 \text{ s}^{-1}$$

$$D_{Nd} = 2.4 \times 10^{-2} \exp(-477 \text{ kJ mol}^{-1}/RT) \text{ m}^2 \text{ s}^{-1}$$

$$D_{Dy} = 7.1 \times 10^{-3} \exp(-461 \text{ kJ mol}^{-1}/RT) \text{ m}^2 \text{ s}^{-1}$$

$$D_{Yb} = 3.2 \times 10^{-1} \exp(-502 \text{ kJ mol}^{-1}/RT) \text{ m}^2 \text{ s}^{-1}.$$

Diffusivities for all of the rare earths investigated in labradorite are similar, in contrast to the significant variations in diffusivities among the rare earths noted in zircon and diopside. This observation is consistent with elastic models for diffusion, in which differences in ionic radii among the rare earths will have greater influence on diffusion rates in stiffer lattices such as those of zircon and clinopyroxene than in the more flexible feldspar structure.

REE diffusion in all of the feldspar compositions is slower than diffusion of divalent and univalent cations, indicating a decrease in diffusion rates with increasing cation charge. Diffusivities of Nd also vary with plagioclase composition, with

* Fax: +1-518-276-6680.

E-mail address: chernd@rpi.edu (D.J. Cherniak).

PII: S0009-2541(02)00246-2

diffusion faster in more sodic plagioclase. This trend is similar to that noted for Sr, Pb and Ba diffusion in previous studies, and may be due to the fact that the comparatively greater flexibility of more sodic plagioclase permits easier migration of diffusants through the mineral lattice.

Keywords: Rare-earth elements; Diffusion; Plagioclase feldspars; Rutherford backscattering

1. Introduction

The process of diffusion plays a significant role in the distribution of trace elements and isotopes within and among minerals in rocks exposed to elevated temperatures for extended periods of time. In previous work on the feldspars, we have measured Sr (Cherniak and Watson, 1992, 1994; Cherniak, 1996), Pb (Cherniak, 1995) and Ba (Cherniak, 2002) in specimens of plagioclase and alkali feldspars over a range of compositions, which has contributed to understanding of the importance of diffusion in influencing measured Sr and Pb isotopes, and the chemical signatures of these elements. In this study, we investigate the diffusion of REE in plagioclase.

While REE concentrations are generally relatively low in feldspars (e.g., Smith and Brown, 1988) with the exception of divalent Eu, the high modal abundance of feldspars in some cases can permit them a role in REE systematics. Further, studies of Nd (and Sr) isotopic zoning in individual feldspar crystals can provide insights into crystallization histories and the evolution of magmas in dynamically mixing systems (e.g., Waight et al., 2000; Bindeman and Bailey, 1999). Hence, it is important to determine the resistance of such zoning to alteration in subsequent thermal events.

In contrast to the cations that we have previously studied, the REE are generally trivalent. By examining a range of REEs, from light (La) to heavy (Yb), we can assess whether diffusion rates differ among them. Although the REEs share similar characteristics, small differences in ionic radii and electronic configurations can lead to pronounced differences in geochemical behavior. Diffusion rates among the rare-earth elements might be influenced by their ionic radii and various crystal-chemical constraints. Such factors appear to significantly affect REE diffusion in zircon (Cherniak et al., 1997a) and diopside (Van Orman et al., 2001), where the LREE diffuse considerably more slowly (and with higher activation energies for diffusion) than the HREE with smaller ionic radii. However, rare-earth elements in calcite (Cherniak, 1998a), yttrium aluminum garnet (Cherniak, 1998b) and apatite (Cherniak, 2000) do not exhibit this systematic variation in diffusivities, although REE diffusion rates are sensitive to the substitutional mechanism in the last case. In aluminosilicate garnets, diffusivities have been found to vary little (Van Orman et al., 2002) or by only a small amount (a factor of $\sim$ 1.8 between Nd and Yb, with the HREE the faster; J. Ganguly, private communication) among the REE.

We can also compare diffusivities of the REE with those of divalent and univalent cations of comparable size, to assess the respective roles of cation size and charge in influencing diffusion rates in feldspars.

Previous work on the diffusion of divalent cations (Sr, Pb, Ba) in plagioclase (Cherniak and Watson, 1992, 1994; Giletti and Casserly, 1994; Cherniak, 1995, 2002) has shown a systematic variation in diffusivities with feldspar composition, with diffusion coefficients increasing with increasing Na content. In this work, we explore the dependence of Nd diffusion rates on plagioclase composition to determine whether this observation applies to diffusion of the REE as well.

2. Experimental procedure

REE diffusion coefficients were determined in three natural plagioclases of differing composition. The feldspars used in this study were an oligoclase (An_{23}) from North Carolina (provided by Don Miller), a labradorite (An_{67}) from Lake County, Oregon, obtained from the collection at the National Museum of Natural History (NMNH #135512-1), and a mega-

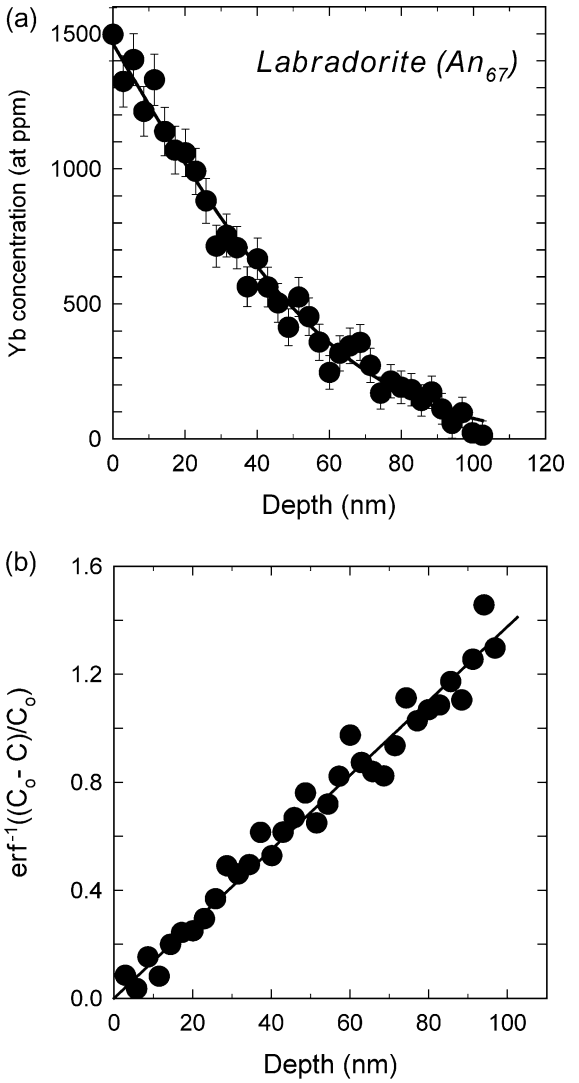

Fig. 1. Typical REE diffusion profile. In this figure, a Yb profile measured in labradorite is shown. In (a), the measured diffusion profile is plotted with the complementary error function solution. In (b), the data are linearized by inversion through the error function. The slope of the line is equal to $(4Dt)^{-1/2}$.

crystic anorthite (An_{93}) from Pacaya Volcano, provided by Don Baker. We have previously measured Sr (Cherniak and Watson, 1992, 1994) and Pb (Cherniak, 1995) diffusion in all three of these feldspars, and Ba diffusion in the oligoclase and labradorite (Cherniak, 2002). Compositional analyses of the plagioclases are presented in Cherniak and Watson (1992, 1994).

For diffusion normal to (010) in all plagioclase compositions, samples were sectioned with a low-speed saw and polished to 0.05-μm gamma alumina. Natural cleavage faces were used in experiments on feldspars in measurements of diffusion normal to (001). All samples were cleaned ultrasonically in distilled water and ethanol, and cut into pieces with surface areas of 10–20 mm^2. Both polished and cleaved samples were then annealed in air at 1000 °C for 48 h. This pre-annealing step serves to anneal possible surface damage produced by cold-working of the polished samples (e.g., Reddy and Cooper, 1982), and to equilibrate point defect concentrations of all samples to conditions that would be similar to those experienced during the experiments.

The sources of REE for the experiments were microcrystalline powders of rare-earth aluminate garnets ($REE_3Al_5O_{12}$) produced by combustion synthesis (Kingsley et al., 1990). Separate source powders were made for each of the four rare earths (La, Nd, Dy and Yb) investigated to avoid interferences in RBS spectra. Experiments were assembled by placing the source mixture (containing a single REE) and a

Table 1
REE diffusion in anorthite and oligoclase

	T (°C)	Time (s)	D (m^2 s^{-1})	log D	+/−
Oligoclase (An_{23})					
Normal to (001)					
NdOlig-4	977	6.05×10^5	1.27×10^{-20}	−19.90	0.09
NdOlig-5	1027	9.43×10^5	1.60×10^{-20}	−19.80	0.04
NdOlig-8	1027	2.59×10^5	1.67×10^{-20}	−19.78	0.15
NdOlig-6	925	5.27×10^6	1.79×10^{-20}	−20.75	0.06
Normal to (010)					
NdOlig-4	977	6.05×10^5	4.74×10^{-21}	−20.33	0.07
NdOlig-5	1027	9.43×10^5	1.76×10^{-20}	−19.75	0.03
NdOlig-8	1027	2.59×10^5	1.58×10^{-20}	−19.80	0.12
NdOlig-6	925	5.27×10^6	7.11×10^{-22}	−21.15	0.06
NdOlig-11	1078	1.62×10^4	1.24×10^{-19}	−18.91	0.12
Anorthite (An_{93})					
NdAnor-4	1349	3.00×10^3	9.33×10^{-19}	−18.03	0.04
NdAnor-3	1300	9.00×10^3	4.22×10^{-19}	−18.38	0.04
NdAnor-2	1250	2.70×10^4	1.03×10^{-19}	−18.99	0.04
NdAnor-1	1200	9.00×10^4	5.77×10^{-20}	−19.24	0.07
NdAnor-6	1150	2.52×10^5	5.60×10^{-21}	−20.25	0.22
NdAnor-7	1100	8.28×10^5	4.20×10^{-21}	−20.38	0.22
NdAnor-8	1050	1.82×10^6	1.34×10^{-21}	−20.87	0.11
NdAnor-5	1000	6.71×10^6	3.25×10^{-22}	−21.49	0.11

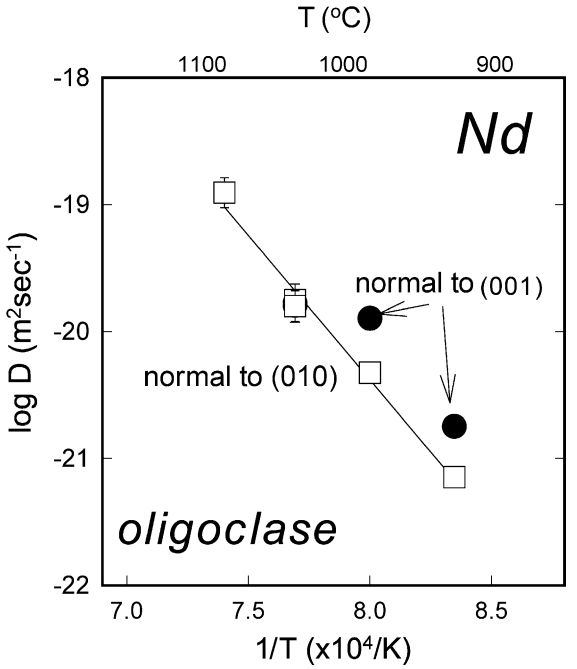

Fig. 2. Arrhenius plot of Nd diffusion in oligoclase. The line is a least-squares fit to the diffusion data normal to (010). For this orientation (with data plotted as open squares), an activation energy of 425 ± 29 kJ mol^{-1} and pre-exponential factor 2.3×10^{-3} m^2 s^{-1} (log $D_o = -2.64 \pm 1.20$) are obtained. Also plotted are data (filled circles) for diffusion normal to (001), which are somewhat faster than diffusion for the (010) orientation.

feldspar specimen in a 5-mm Pt capsule. After loading, the Pt capsules were crimped shut.

Prepared sample capsules were annealed in 1-atm furnaces at temperatures from to 925 to 1350 °C for times ranging from 35 min to 2 months. Temperatures in the experiments under 1100 °C were monitored with type K (chromel–alumel) thermocouples during the course of the anneals; temperature uncertainties are ±2 °C. A type S (Pt–Pt10%Rh) thermocouple was used for the higher-temperature runs, with comparable temperature uncertainty. On completion of the anneals, samples were quenched by removing them from furnaces and permitting them to cool in air. Samples were then removed from capsules and cleaned ultrasonically in successive baths of distilled water, and ethanol. The samples were readily removed from the source material and sample surfaces using these sources are easily cleaned of the residue, as was the case for sources used in our Sr diffusion studies (Cherniak and Watson, 1992, 1994; Cherniak, 1996).

A "zero-time" experiment was also run at 1200 °C for the labradorite. For this experiment, the sample capsule was prepared as above, placed in the furnace, brought up to run temperature, and immediately quenched.

3. RBS analysis

RBS has been used in our measurements of Pb and Sr diffusion in feldspars (Cherniak and Watson, 1992, 1994; Cherniak, 1995, 1996) and in many other diffusion studies. The experimental and analytical approaches used here are similar to those used in our previous work. Helium beam energies used ranged between 1.5 and 2 MeV, with incident energies in the lower range used for some analyses in order to

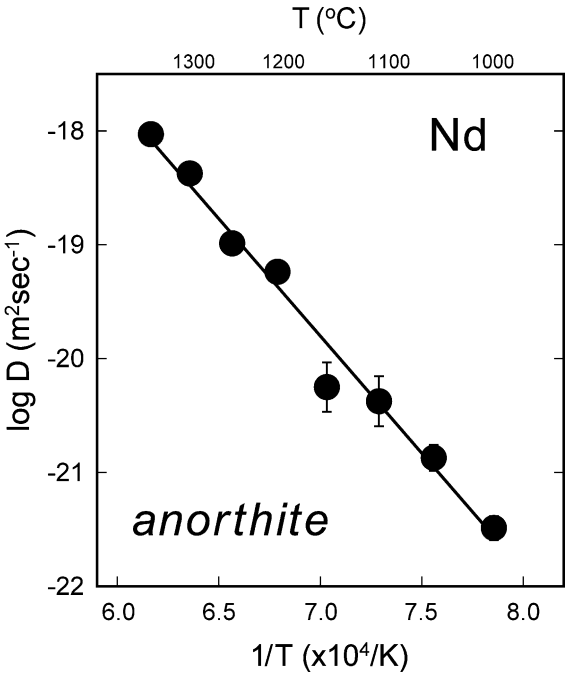

Fig. 3. Arrhenius plot for Nd diffusion in anorthite. From a fit to the diffusion data, we obtain an activation energy of 398 ± 22 kJ mol^{-1} and pre-exponential factor 5.9×10^{-6} m^2 s^{-1} (log $D_o = -5.23 \pm 0.82$) for diffusion normal to (010).

improve sensitivity. Spectra were converted to REE concentration profiles employing procedures outlined in previous work. The data analysis routine used to extract depth scales from the raw data took into account the compositional differences of the feldspars employed in these experiments, and the effect of this variation on stopping powers for the helium ions. The resultant profiles (concentration vs. depth) were fit to the solution of a diffusion equation to determine the diffusion coefficient (D). The diffusion equation chosen describes simple one-dimensional, concentration-independent diffusion in a semi-infinite medium with a source reservoir maintained at constant concentration (i.e., a complementary error function solution). The rationale for the use of this model has been addressed elsewhere (e.g., Cherniak and Watson, 1992, 1994). Diffusivities are evaluated by plotting the inverse of the error function (i.e., $\mathrm{erf}^{-1}((C_o - C(x,t))/C_o)$) vs. depth ($x$) measured from the sample surface. If the data fit the solution defined by the model, a straight line with slope $(4Dt)^{-1/2}$ is obtained. C_o, the surface concentration of diffusant, is determined by iteratively varying its value until the intercept of the line converges on zero. In Fig. 1, a typical diffusion profile and its inversion through the error function is shown. The uncertainties in concentration and depth from each data point (mainly derived from counting statistics in the former and detector resolution in the latter) were used in evaluating the uncertainties in the diffusivities determined from fits to the model solution.

4. Results

The results for Nd diffusion experiments on oligoclase are presented in Table 1 and plotted in Fig. 2. For diffusion normal to (010), an activation energy of 425 ± 29 kJ mol^{-1} and pre-exponential factor of 2.3×10^{-3} m^2 s^{-1} ($\log D_o = -2.64 \pm 1.20$) are obtained. Rates for diffusion normal to (001) are somewhat faster (by about 0.5 log unit) than those for diffusion normal to (010), behavior similar to that observed for Pb and Ba diffusion in oligoclase (Cherniak, 1995, 2002).

The Nd diffusion results for anorthite are presented in Table 1 and plotted in Fig. 3. From a fit of these data, we obtain an activation energy of 398 ± 22 kJ mol^{-1} and pre-exponential factor of 5.9×10^{-6} m^2 s^{-1} ($\log D_o = -5.23 \pm 0.82$).

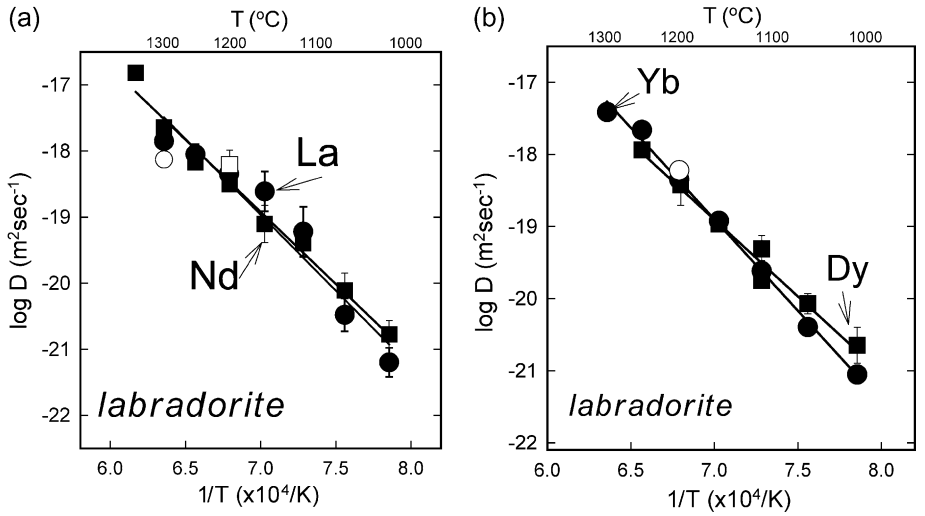

Fig. 4. Arrhenius plots of REE diffusion data for labradorite. In (a), data for La and Nd diffusion are plotted. From the least-squares fit to the La diffusion data, an activation energy of 464 ± 50 kJ mol^{-1} and pre-exponential factor 1.1×10^{-2} m^2 s^{-1} are obtained. Arrhenius parameters for Nd are 477 ± 47 kJ mol^{-1} and 2.4×10^{-2} m^2 s^{-1} for diffusion normal to (010). In (b), data for Dy and Yb are shown. From the least-squares fit to the Dy diffusion data, an activation energy of 461 ± 23 kJ mol^{-1} and pre-exponential factor 7.1×10^{-3} m^2 s^{-1} are obtained. Arrhenius parameters for Yb are 502 ± 14 kJ mol^{-1} and 3.2×10^{-1} m^2 s^{-1} for diffusion normal to (010). Diffusivities for transport normal to (001) (open symbols) are similar to D for the (010) orientation (filled symbols) for all of the REE.

Results from diffusion measurements on labradorite for the four rare earths La, Nd, Dy and Yb are plotted in Fig. 4 and presented in Table 2. For diffusion normal to (010), we obtain the following Arrhenius parameters:

La—$E_a = 464 \pm 50$ kJ mol^{-1};
$D_o = 1.1 \times 10^{-2}$ m^2 s^{-1} ($\log D_o = -1.96 \pm 1.87$)

Nd—$E_a = 477 \pm 47$ kJ mol^{-1};
$D_o = 2.4 \times 10^{-2}$ m^2 s^{-1} ($\log D_o = -1.62 \pm 1.77$)

Dy—$E_a = 461 \pm 23$ kJ mol^{-1};
$D_o = 7.1 \times 10^{-3}$ m^2 s^{-1} ($\log D_o = -2.15 \pm 0.87$)

Yb—$E_a = 502 \pm 14$ kJ mol^{-1};
$D_o = 3.2 \times 10^{-1}$ m^2 s^{-1} ($\log D_o = -0.49 \pm 0.52$)

Measurements of diffusion normal to (001) indicate little anisotropy for REE diffusion in labradorite.

The "zero-time" experiment with the labradorite, as well as a time-series study for Dy diffusion at 1100 °C, were performed in order to verify that the measured concentration profiles represent volume

Table 2
REE diffusion in labradorite (An_{67})

	T (°C)	Time (s)	D (m^2 s^{-1})	log D	+/−
Dy					
Normal to (010)					
DyLab-2	1250	6.84×10^4	1.15×10^{-18}	−17.94	0.05
DyLab-1	1198	1.69×10^5	1.08×10^{-19}	−18.42	0.28
DyLab-5	1150	3.73×10^5	3.76×10^{-19}	−18.97	0.09
DyLab-6	1100	6.01×10^5	1.79×10^{-20}	−19.75	0.04
DyLab-10	1100	2.30×10^5	4.93×10^{-20}	−19.31	0.19
DyLab-9	1100	5.76×10^4	2.19×10^{-20}	−19.66	0.19
DyLab-7	1050	9.05×10^5	8.48×10^{-21}	−20.07	0.14
DyLab-8	1000	1.27×10^6	2.25×10^{-21}	−20.65	0.25
Nd					
Normal to (001)					
NdLab-2	1199	7.56×10^4	5.58×10^{-19}	−18.25	0.04
Normal to (010)					
NdLab-5	1348	2.10×10^3	1.52×10^{-17}	−16.82	0.03
NdLab-4	1300	5.40×10^3	2.29×10^{-18}	−17.64	0.08
NdLab-3	1250	2.16×10^4	6.71×10^{-19}	−18.17	0.04
NdLab-2	1199	7.56×10^4	3.15×10^{-19}	−18.50	0.07
NdLab-6	1150	3.73×10^5	7.85×10^{-20}	−19.11	0.28
NdLab-7	1100	6.01×10^5	4.02×10^{-20}	−19.40	0.10
NdLab-8	1050	9.05×10^5	7.80×10^{-21}	−20.11	0.26
NdLab-9	1000	1.27×10^6	1.68×10^{-21}	−20.77	0.21
La					
Normal to (010)					
LaLab-3	1300	5.40×10^3	1.42×10^{-18}	−17.85	0.27
LaLab-2	1250	2.16×10^4	8.89×10^{-19}	−18.05	0.15
LaLab-1	1198	8.58×10^4	4.52×10^{-19}	−18.35	0.07
LaLab-7	1150	2.20×10^5	2.44×10^{-19}	−18.61	0.30
LaLab-6	1100	6.01×10^5	6.00×10^{-20}	−19.22	0.37
LaLab-8	1050	1.61×10^6	3.32×10^{-21}	−20.48	0.23
LaLab-9	1000	1.49×10^6	6.32×10^{-22}	−21.20	0.18
Normal to (001)					
LaLab-1	1198	8.58×10^4	6.22×10^{-18}	−18.21	0.02
Yb					
Normal to (010)					
YbLab-3	1300	5.40×10^3	3.87×10^{-18}	−17.41	0.07
YbLab-2	1250	2.16×10^4	2.18×10^{-18}	−17.66	0.03
YbLab-1	1198	8.58×10^4	4.50×10^{-19}	−18.35	0.02
YbLab-5	1150	3.73×10^5	1.19×10^{-19}	−18.92	0.04
YbLab-6	1100	6.01×10^5	2.42×10^{-20}	−19.62	0.04
YbLab-7	1050	1.61×10^6	4.04×10^{-21}	−20.39	0.05
YbLab-8	1000	1.49×10^6	8.86×10^{-22}	−21.05	0.10
Normal to (001)					
YbLab-1	1198	8.58×10^4	6.02×10^{-19}	−18.22	0.04

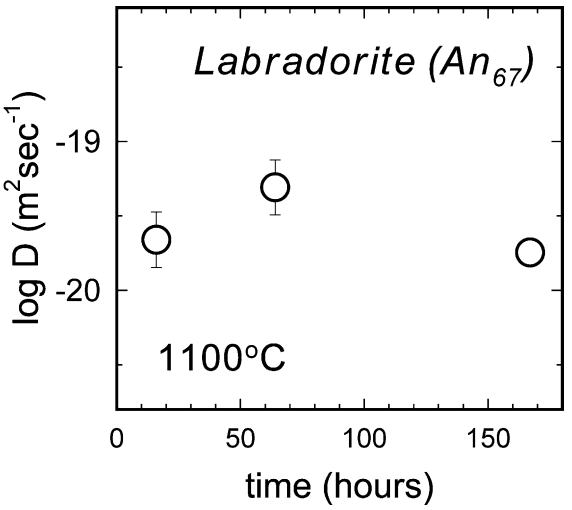

Fig. 5. Results from a time series for Dy diffusion in labradorite, with experiments run at 1100 °C. Diffusion rates are quite similar, despite differences in anneal times ranging over about an order of magnitude (from 1.7 to 16 h), suggesting that the dominant process being measured is volume diffusion.

diffusion and are not a result of other phenomena such as surface reaction that may otherwise result in enhanced REE concentration in the near-surface region. The "zero-time" anneal also serves to highlight possible systematic problems in the experimental approach. In Fig. 5, the results from the time series at 1100 °C are plotted. Diffusivities at this temperature are quite similar for times ranging over more than an order of magnitude, suggesting that volume diffusion is the dominant contributor to the observed diffusion profiles. The zero-time experiment (not shown) displays little evidence of significant near-surface REE during the heat-up and quench phases of the anneal, offering further confirmation that measured REE profiles are a consequence primarily of lattice diffusion.

5. Discussion

5.1. Effect of feldspar composition on diffusivities

Arrhenius relations for Nd diffusion in the investigated feldspar compositions are shown in Fig. 6. The data clearly indicate that diffusion rates are higher for more sodic plagioclase, a finding consistent with observations for the divalent cations Sr (Cherniak and Watson, 1994; Giletti and Casserly, 1994), Pb (Cherniak, 1995) and Ba (Cherniak, 2002). For diffusion normal to (010), Nd diffusion in anorthite is about an order of magnitude slower than in labradorite; diffusion of Nd in oligoclase is about three-quarters of a log unit faster. Activation energies for REE diffusion are comparable for all plagioclase compositions investigated.

5.2. Comparison of diffusivities among the REE

The range of rare-earth elements investigated in labradorite in this study permits us to explore whether diffusivities vary among the REE in feldspar. In other diffusion studies, it has been observed that diffusivities vary systematically with ionic radius across the range of REEs for both clinopyroxene (Van Orman et al., 2001) and zircon (Cherniak et al., 1997a), with the smaller HREE having faster diffusion rates than the larger LREE. In contrast, little variation in diffusivities among the REE have been noted in calcite (Cherniak, 1998a), aluminosilicate (Van Orman et al., 2002) and aluminate (Cherniak, 1998b) garnets, or apatite (Cherniak, 2000).

Labradorite resembles this latter group of minerals in that there appears to be little variation among diffusivities of the rare-earth elements investigated (Fig. 7). Differences in behavior among these groups of minerals may be in part a consequence of their elastic properties. Both zircon and diopside have relatively rigid lattices for which relative differences in cationic radii of like-charged species are likely to be a more critical factor in influencing diffusivities. The differences among the diffusion rates for the REE are in fact most pronounced for minerals with larger elastic moduli (e.g. zircon). However, even among minerals with smaller elastic moduli, differences in diffusivities among like-charged cations can be significant if differences in ionic radii are large, as is the case for Ca vs. Ba and Na vs. K in feldspars, where these differences are 0.35 and 0.36 Å, respectively.

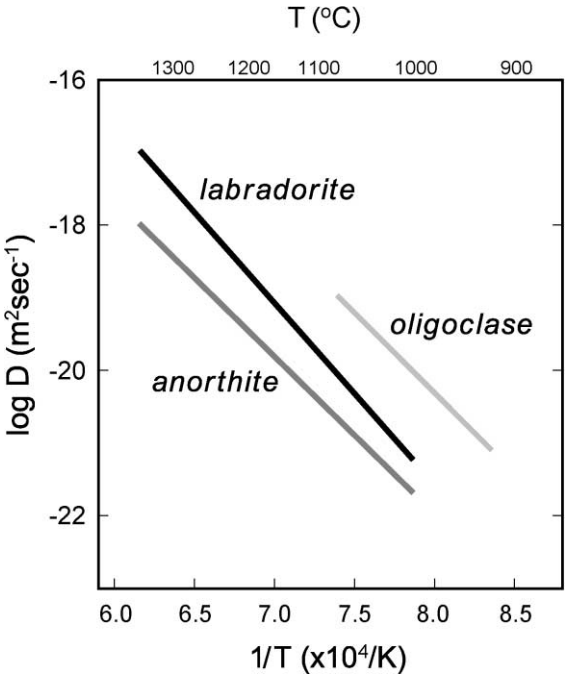

Fig. 6. Summary of Nd diffusion data (diffusion normal to (010)) for plagioclase compositions investigated in this work. Diffusion is faster for the more sodic oligoclase, a finding consistent with previous work on diffusion of divalent cations.

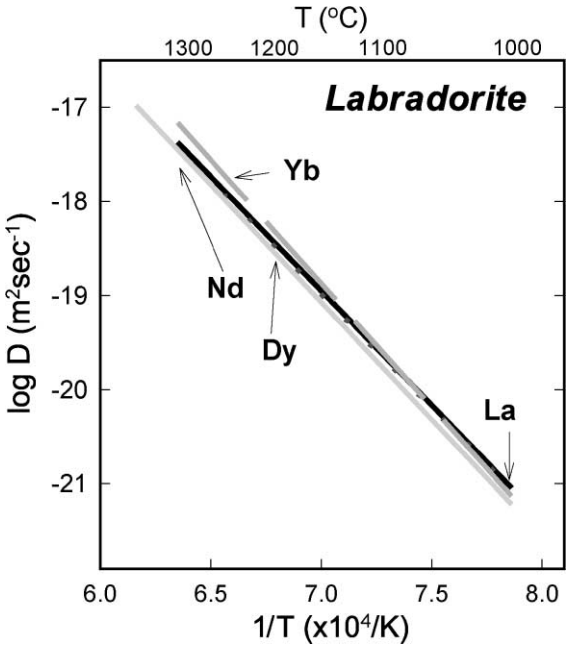

Fig. 7. Arrhenius plot comparing diffusivities of the rare earths La, Nd, Dy and Yb in labradorite. There is relatively little difference in diffusion rates among the REE.

These large variances can be contrasted with the difference of 0.16 Å between the radii of La and Yb (all for sixfold coordination, Shannon, 1976), and are discussed in the following section.

5.3. Comparison with diffusivities of other cations in feldspar

Plots of diffusion data for various cations in the plagioclase compositions studied are presented in Fig. 8. Diffusion of several divalent and univalent cations has been measured in labradorite (Fig. 8a). Behrens et al. (1990) have measured Ca diffusion using a ^{45}Ca tracer, while Cherniak and Watson (1994) and Cherniak (1995, 2002) have measured Sr, Pb and Ba diffusion, respectively, in labradorite from the same locality. Giletti and Shanahan (1997) have measured K and Na diffusion in labradorite. A clear dependence of diffusion rates on both cation size and charge can be seen. Diffusion of the univalent cations is faster than diffusion of the divalent cations, which in turn are faster than diffusion of the REE. For cations of comparable size, the trend of slower D and higher activation energy for diffusion with increasing charge is evident (Fig. 9). To first-order approximation, the change in electrostatic energy as an ion moves from one position of equilibrium to another (which is related to the activation energy) in a solid is linearly dependent upon the magnitude of the cation charge (e.g., Anderson and Stuart, 1954). Higher activation energies and slower overall diffusion rates with increasing cation charge are also observed for the other plagioclase compositions investigated, as noted below.

In groups of like-charged cations, there is also a trend of slower D with increasing ionic radius. For example, Ca diffusion is about two orders of magnitude faster than Ba diffusion [ionic radii of 1.35 Å for Ba vs. 1.00 Å for Ca (Shannon, 1976) in sixfold coordination (Smyth and Bish, 1988)]. Diffusion of Sr and Pb are also faster than Ba, and they diffuse slightly slower than Ca, a reasonable finding given their intermediate ionic radii (1.18 and 1.19 Å for Sr and Pb, respectively). However, both Pb and Sr diffusion exhibit some anisotropy, with diffusion normal to (001) faster than diffusion normal to (010) by about 0.7 log unit. The dependence of diffusion rate on size has also been shown for univalent cations in labradorite (Giletti and Shanahan, 1997), with Na (1.02 Å) diffusing at a rate two to three orders of magnitude faster than K (1.38 Å); these univalent cations differ in size by an amount comparable to that separating the divalent cations Ba and Ca. As earlier noted, however, there is little difference in diffusivities among the trivalent REE. Part of this may be due to the less dramatic variations in ionic radii across the REE and the relatively more flexible structure of the feldspars. It may also be that these differences become less pronounced with higher cationic charge, as has been observed in zircon. In the case of zircon, both diffusivities and activation energies for diffusion differ more dramatically among the REE than among tetravalent cations (Cherniak et al., 1997a,b).

In oligoclase, the trends noted for labradorite also broadly apply (Fig. 8b), although there is also evidence of anisotropy in diffusion of large divalent cations, as well as for the REE. In anorthite (Fig. 8c), only diffusion of divalent cations has been measured, but there is some correlation of cation size and diffusion rates among these (e.g., LaTourette and Wasserburg, 1998; Giletti and Casserly, 1994; Cherniak, 1995; Cherniak and Watson, 1992).

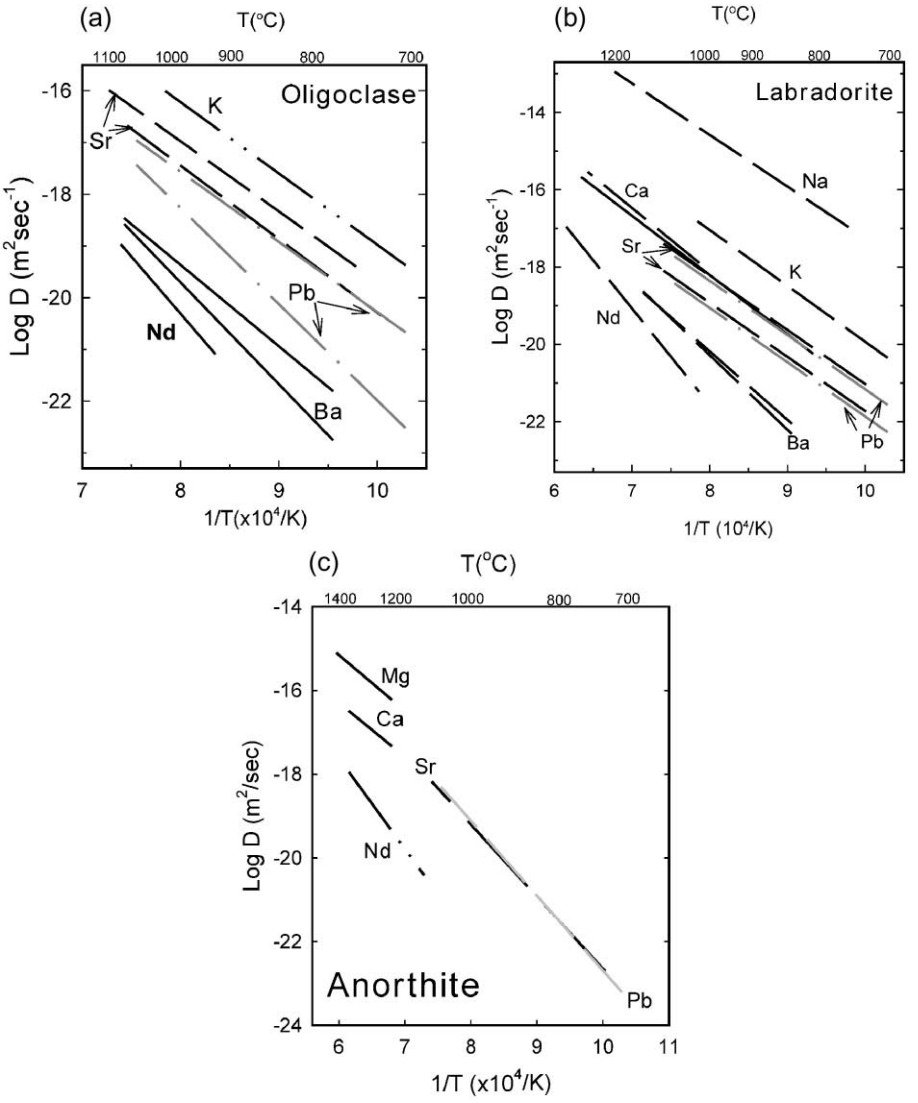

Fig. 8. Summary of cation diffusion data for the three feldspar compositions: (a) oligoclase; (b) labradorite; (c) anorthite. Sources for data: Ca in labradorite—Behrens et al. (1990); Sr in oligoclase and labadorite—Cherniak and Watson (1994); Sr in anorthite—Cherniak and Watson (1992); Pb in oligoclase, labadorite and anorthite—Cherniak (1995); K in oligoclase and Na and K in labradorite—Giletti and Shanahan (1997); Ca and Mg in anorthite—LaTourette and Wasserburg (1998); Ba in oligoclase and labradorite—Cherniak (2002); Nd—this study.

These observations are in accord with the conclusion that elastic properties of the crystal lattice have important influences on diffusion. Minerals with larger Young's moduli generally exhibit larger activation energies for diffusion, and consequent lower diffusivities. These minerals also tend to show stronger dependencies of diffusion on cation size and charge. Elastic properties have been shown to influence partitioning behavior in plagioclase (Blundy and Wood, 1991), where the more flexible sodic plagioclase structure accommodates Sr and Ba ions more readily than does the more rigid calcic plagioclase. Similar intuitive reasoning can be applied to diffusional behavior if we conjecture that a more flexible (i.e., smaller elastic modulus) structure would also permit easier cation migration, and is consistent with

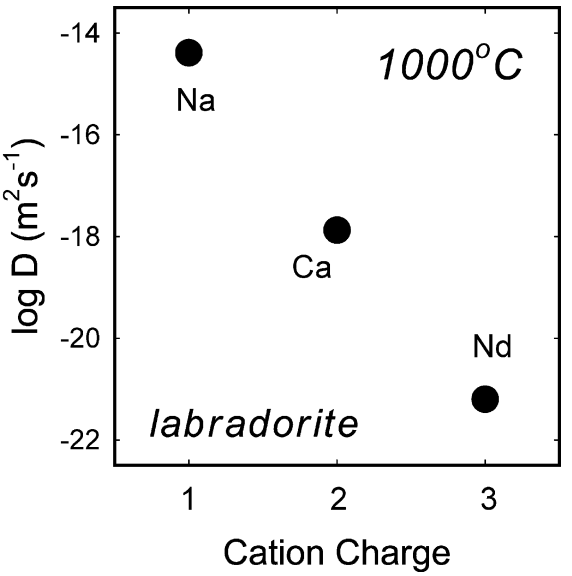

Fig. 9. Plot of diffusion coefficients for diffusion at 1000 °C in labradorite for three cations of comparable sizes (Na, Ca and Nd) but differing charges (1+, 2+ and 3+, respectively). A systematic increase in D with decreasing charge can be noted, consistent with the first-order linear dependence expected given simple electrostatic energy considerations.

our observations of faster cation diffusivities with increasing Na content of plagioclase. It should be noted, however, that the Blundy and Wood model introduces the concept of Young's modulus for the site filled by the substituent impurity ion, rather than the site as occupied by the major constituent species. While this may be meaningful in treating equilibrium partitioning of elements, where the primary consideration is incorporation of the impurity on a specific lattice site, it is not clear whether this is the appropriate parameter in the case of diffusion, since ions must travel through the material and occupy intermediate positions en route to specific lattice sites. It seems more likely that the transport properties would in some way reflect the bulk elastic property of the material through which diffusion occurs.

We can attempt to describe these diffusion behaviors, at least qualitatively, with a simple elastic model for diffusion (Van Orman et al., 2001). This model, adapted from the work of Mullen (1966) and Zener (1952), assumes that the motion energy of diffusing ions is due to elastic strain, and considers the difference in motion energy that results from the difference between the size of an impurity ion and the ideal site radius. This quantity, expressed as a size factor δ, where $\delta=(r_{imp}-r_{site})/r_o$ with r_{imp}, the impurity ion radius, r_{site}, the ideal site radius and r_o, the average cation–anion distance. Activation energies for diffusion may be larger for cations larger than the ideal size. A relationship relating the diffusivities themselves to ion size can be derived if one assumes that a large proportion of the energy expended in an atomic jump is due to lattice strain. In the pre-exponential factor, D_o, only motion entropy [as it depends on the elastic stress field set up by the defect (e.g., Shewmon, 1989; Zener, 1952)] and jump frequency depend on the type of diffusing ion rather than the lattice itself. If it is assumed that differences in jump frequencies among like-charged cations are small, then the log of D_o will be proportional to the motion entropy, S_m, which will be dependent on the temperature derivative of the material's bulk modulus (μ). Cation size can then be related to diffusion coefficient as follows:

$$\ln D \approx \ln D^{\delta=0} - \frac{2E_m^o}{R}\left[\frac{\partial(\mu/\mu_o)}{\partial T}+\frac{1}{T}\right] \times \left[\delta\left(1-1/\sqrt{2}\right)^{-1}-\delta^2\left(1-1/\sqrt{2}\right)^{-2}\right]. \quad (1)$$

This equation describes a parabola, with a minimum value when $\delta = 0.146$. Using this expression, the minimum diffusivity for labradorite will occur for an ionic radius of 0.160 nm; for the less rigid structure of oligoclase, it will be 0.165 nm, and 0.157 nm for the more rigid anorthite. However, it is counterintuitive to assume that diffusivities will increase with increasing ionic radius beyond this minimum; the data presented here explore only the region where $\delta < \delta_{min}$, so we can offer no comment on the diffusional behavior of cations beyond this size limit. Because the width of the parabola is a function of the temperature derivative material's bulk modulus, the feldspar curves will slope more gently from the minimum, with less dramatic variations in diffusivities with ionic radius than in the case of more rigid lattices such as zircon and clinopyroxene.

We can also consider the relationship between diffusion coefficient and ionic charge in the context of this model. Differences in charge can be incorporated in the above expressions by considering the

motion energy proportional to cation charge, and motion energy and entropy linearly related. If we consider the case of a single material, $(E^{o}_{m}/R)[\partial(\mu/\mu_{o})/\partial T+1/T]$ will be the same; the size factor δ will also be the same for cations of comparable ionic radius. We then obtain the expression:

$$\ln D_z \approx \ln D^{\delta=0}_{z_{ref}} + K_1\left(1-\frac{z}{z_{ref}}\right) - 2K_1\left(\frac{z}{z_{ref}}\right)K_2 \quad (2)$$

where $K_1=(E^{o}_{m}/R)[\partial(\mu/\mu_{o})/\partial T+1/T]$ and $K_2=[\delta(1-1/\sqrt{2})^{-1}-\delta^2(1-1/\sqrt{2})^{-2}]$. This simple linear dependence of ln D on cation charge z is consistent with what we observe for cations of similar size but differing charge (Fig. 9).

5.4. Geological applications

5.4.1. Preservation of Nd zoning

REE abundances are generally low in most plagioclases, with the exception of Eu^{2+} (e.g., Smith and Brown, 1988). Nonetheless, we can briefly explore the ways in which the signatures of trivalent REEs in feldspars might be altered by diffusion and affect whole-rock REE systematics. Nd isotope zoning in feldspar grains can record isotopic change in magmatic systems and provide insight into magma mixing processes. Nd has been observed to exhibit significant compositional zoning in feldspar phenocrysts, which can be useful in assessing geochemical evolution in magmatic systems (e.g., Waight et al., 2000). Simple calculations can be used to determine which conditions permit such zoning to be lost. We consider a model with zones of 100 μm width. Zones in a feldspar are modeled as plane sheets of thickness l; adjacent planes have different concentrations of diffusant, and concentrations within a zone are initially uniform. Only isothermal diffusion normal to the planar interface is considered. Two (somewhat arbitrary) criteria for alteration of zones is employed. Zones are considered to be "lost" if a compositional change of 10% is attained in the zone's center, and "blurred" when there is an equivalent compositional change 10% of the way into the zone. The dimensionless parameter Dt/l^2 will be equal to 3.3×10^{-2} when the former condition occurs, and 1.8×10^{-3} when the latter prevails (Crank, 1975). Fig. 10 shows curves constraining the time–temperature conditions under

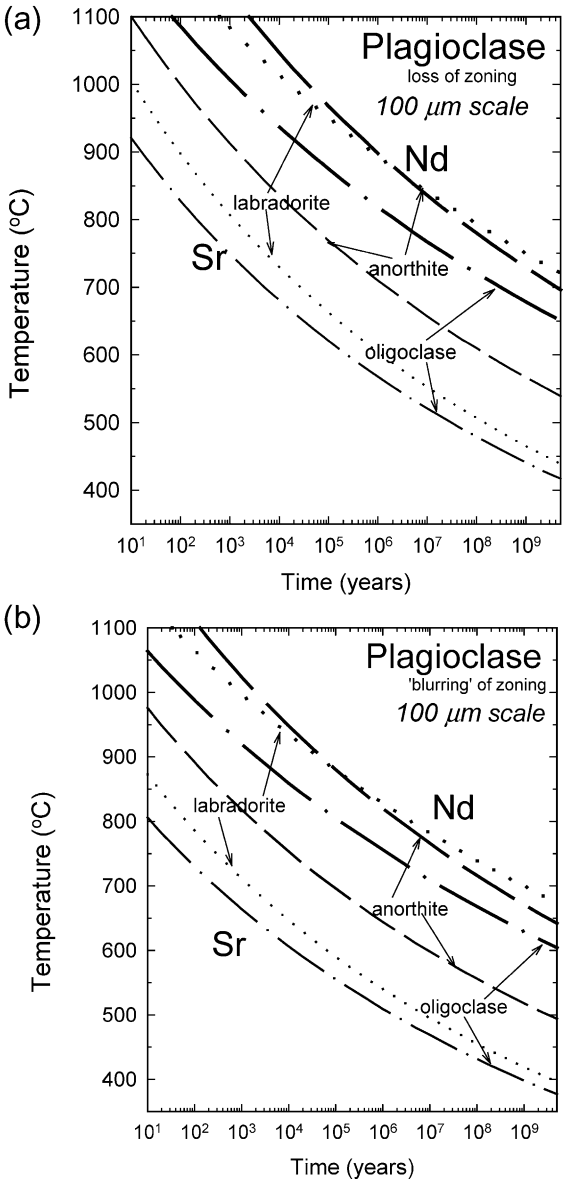

Fig. 10. Preservation of Nd and Sr zoning in feldspar. Curves (thick lines for Nd, finer lines for Sr) represent maximum time–temperature conditions under which 100-μm zoning in these elements will be preserved in anorthite, labradorite and oligoclase. In (a), well-defined zoning will be lost for conditions above the curves in each group. For conditions in (b), zones will be "blurred" at edges but will not be completely obliterated.

which Nd (and Sr) zoning of these dimensions will be retained in anorthite, labradorite and oligoclase given the above criteria. At 750 °C, for example, labradorite

and anorthite 100-μm scale zoning in Nd would resist obliteration for about a billion years, with zoning in oligoclase persisting for ~ 20 Ma. If Sr zoning on the same scale exists, it will be lost more readily; at this temperature, 100-μm Sr zoning will be retained for 200,000, 5000 and 1000 years for anorthite, labradorite and oligoclase, respectively.

Zoning on this scale would obviously be "blurred" under less extreme time–temperature conditions. For example, Nd compositional "blurring" of 100-μm zones in 1 million years would require temperatures of ~ 825 °C for labradorite and anorthite and ~ 750 °C for oligoclase; zoning of Sr would be "blurred" at temperatures of ~ 640, ~ 540 and ~ 510 °C for anorthite, labradorite and oligoclase, respectively. Again, it is evident that Sr isotope signatures are much more likely to be altered by diffusion than are those of the REE.

It should be pointed out that these calculations apply only for trivalent REE. Given the preceding discussion regarding the role of cation size and charge in influencing diffusivities in feldspars, it can be argued (although it has not been measured directly) that the diffusion rates for divalent Eu should be similar to those for Sr^{2+}, considering their comparable ionic radii (1.17 vs. 1.18 Å; Shannon, 1976).

5.4.2. Diffusive re-equilibration of melt inclusions

Cottrell et al. (in press) have developed a numerical model to explore the effects of diffusion in a crystal host on the composition of melt inclusions. They consider the compositional evolution of a spherical melt inclusion contained within a crystal with which it is initially out of equilibrium (the end-member case), and evaluate the effects of partition coefficients, diffusivities, and inclusion size on the rate of re-equilibration. We can use our diffusion data with this model to show the degree of re-equilibration of inclusions of various size with a host plagioclase. In this example, we use a partition coefficient for Nd between plagioclase and melt of 0.9 (e.g., Bindeman et al., 1998), and the diffusivity for Nd in anorthite (at 1200 °C) obtained in the present study. In Fig. 11, the degree of re-equilibration (1 for complete equilibration of inclusion with the crystal) is shown as a function of time for inclusions of 10-, 50- and 200-μm radii. This process can be quite rapid at high temperatures; a 50-μm radius inclusion would be about 90% of the way toward equilibration with its host in about 5000 years.

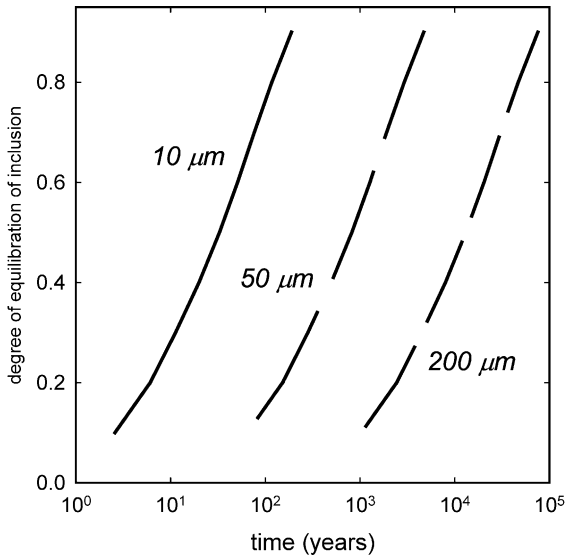

Fig. 11. Degree of equilibration of melt inclusions with host plagioclase, using the model of Cottrell et al. (in press). Curves show extent of equilibration of Nd as a function of time for three different inclusion radii (10, 50 and 200 μm). Further details are provided in the text.

The model also permits examination of the effects of the inclusion on the trace element composition of the crystal host. We again use Nd in anorthite as an example. In Fig. 12, the width (as measured from the rim of the inclusion) of the diffusion "halo" in the crystal surrounding the inclusion is shown as a function of time for three temperatures. This distance is defined as the position at which the concentration is 95% of the difference between the Nd concentration of the inclusion and the initial Nd concentration of the crystal. In these calculations, a 50-μm radius inclusion is used, the same partition coefficient as above, and the diffusivities for Nd in anorthite as determined in this study. A halo of 100 μm width would be produced in about 15,000 years at 1100 °C, and in a time about an order of magnitude shorter at 1200 °C.

5.4.3. Sm–Nd isotope constraints on planetary differentiation and thermal histories

Sm–Nd data from plagioclase inclusions in iron meteorites have been used to constrain thermal histories and better understand planetary differentiation

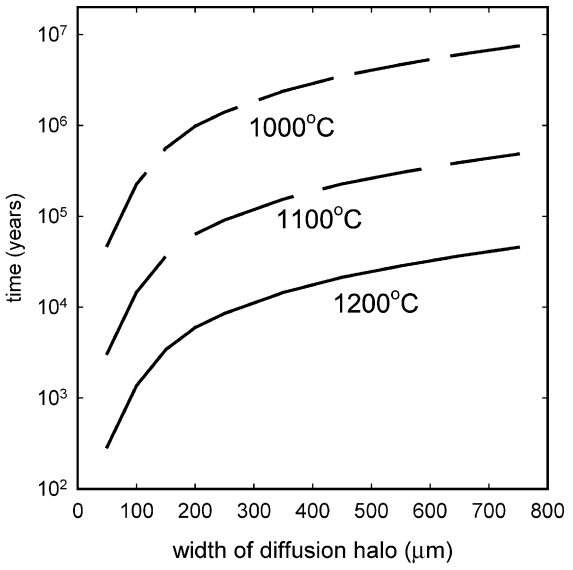

Fig. 12. Size of diffusion "halos" in plagioclase host surrounding a melt inclusion (defined as the position at which the concentration is 95% of the difference between the Nd concentration of the inclusion and initial Nd concentration of the feldspar). The growth of halo widths with time is calculated for three different temperatures (1000, 1100 and 1200 °C). Additional details are provided in the text.

processes (Stewart et al., 1994, 1996). They consider the conditions under which magmatic Sm–Nd ages are preserved when the silicate phase is mixed with molten FeNi metal, and derive an expression to approximate the degree of isotopic equilibration (E_f):

$$E_f \approx \frac{1.1x}{a}\left(\frac{D(T_o)}{\kappa}\right)^{1/2} \quad (3)$$

where x is the depth of burial of the silicate, a is the grain radius, $D(T_o)$ is the diffusivity at the temperature at which cooling begins, and κ is the thermal diffusivity of the burial medium (which can be composed of silicate or metallic material). Because of the paucity of REE diffusion data for plagioclase at the time, the authors used Sr diffusion parameters from our earlier work (Cherniak and Watson, 1994) to estimate Sm–Nd diffusivities. However, measurements in the present study indicate that Nd diffusion is fully two orders of magnitude slower than Sr diffusion at 1200 °C, which means that burial depths of silicate inclusions could be up to an order of magnitude greater and still preserve Nd isotopic signatures.

In a recent paper, Ganguly and Tirone (2001) have considered the problem of the Morristown mesosiderite meteorite, in which an age discrepancy exists between mesosiderite Pb–Pb ages and the Morristown's Nd–Sm age, with the latter 90 Ma younger. In an attempt to explore whether this discrepancy might be due to resetting of the Sm–Nd system during cooling rather than "impulsive" disturbance (e.g., Prinzohofer et al., 1992), they calculated the relative times for closure of the Sm–Nd system to diffusive exchange in both plagioclase and orthopyroxene during cooling. In their calculations, they assumed Arrhenius parameters for Nd diffusion in calcic plagioclase of 247 kJ mol^{-1} for the activation energy, and 2.5×10^{-10} m^2 s^{-1} for the pre-exponential factor. This would yield a diffusivity for Nd of 4.7×10^{-22} at 827 °C, or about a factor of 2 slower than the Nd diffusion coefficient (1.1×10^{-21} m^2 s^{-1}) measured in one experiment on orthopyroxene (with composition $En_{96}Fs_1$) conducted at this temperature by Ganguly and Tirone (2001).

However, the diffusivity calculated for Nd in anorthite using the Arrhenius parameters from the present work is about three orders of magnitude smaller (7.7×10^{-25} m^2 s^{-1}) at this temperature. With this slower diffusivity, using the same time constant and grain size as in the Ganguly and Tirone (2001) calculations, the time to closure of plagioclase to Nd exchange would be considerably shorter, only a few Ma, than the many tens of Ma calculated for plagioclase by Ganguly and Tirone (2001), and also much shorter than the time to closure for orthopyroxene (~ 50–90 Ma) determined in their study. The present diffusion results, therefore, suggest that other explanations may need to be considered to account for the observed age discrepancy in the Morristown mesosiderite.

6. Closure temperatures

A summary of diffusion data for the REE in various minerals is shown in Fig. 13. REE diffusivities for feldspars are intermediate among those minerals for which diffusion data exist, faster than in zircon, but slower than diffusion in apatite, calcite and fluorite. REE diffusion in plagioclase falls in the same range as REE diffusion in titanite and middle to heavy

REE diffusion in clinopyroxene. However, Nd and other LREE diffuse significantly more slowly in clinopyroxene than Nd in plagioclase. At 1200 °C, for example, Nd diffuses more than an order of magnitude faster in anorthite than in diopside (Van Orman et al., 2001); these differences increase for more sodic plagioclase, with Nd diffusion two orders of magnitude faster in labradorite than in diopside, and Nd diffusion in oligoclase nearly 700 times faster than in diopside at 1200 °C. This is consistent with the arguments of Prinzohofer et al. (1992) that Sm–Nd systematics in plagioclase are much more likely to be disturbed than those of coexisting clinopyroxene in metamorphosed meteorites.

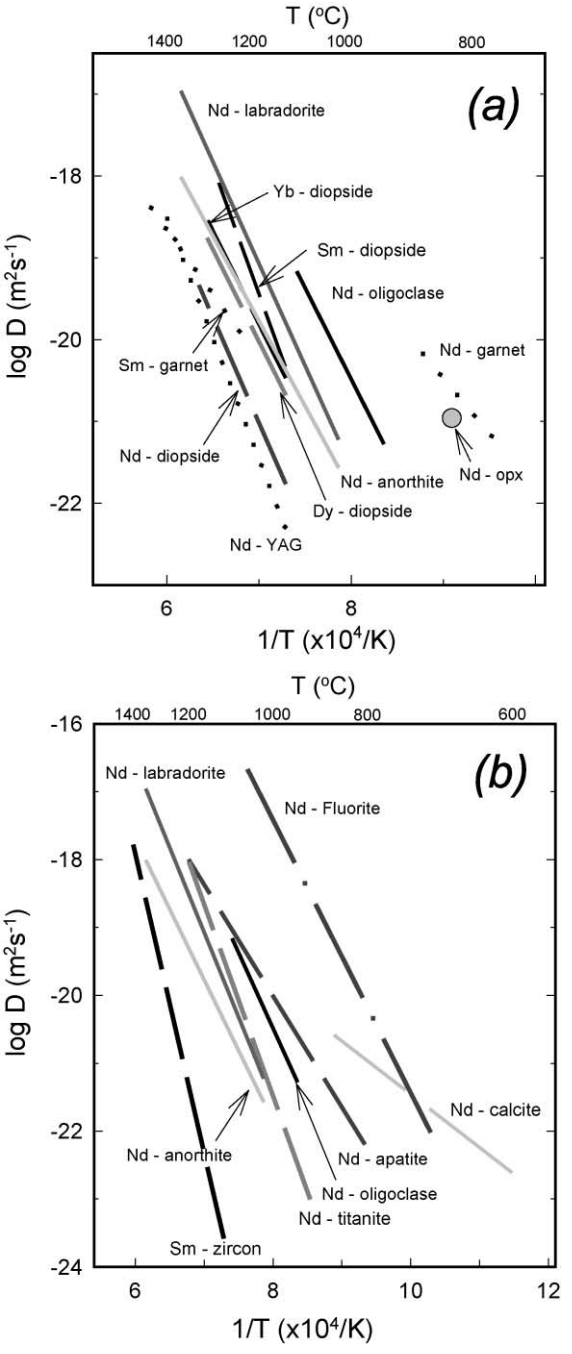

These differences in diffusivities are reflected in calculated closure temperatures for the REE. Closure temperatures are frequently calculated using the formalism of Dodson (1973):

$$T_c = \frac{E_a/R}{\ln\left(\frac{ART_c^2 D_o/a^2}{E_a \mathrm{d}T/\mathrm{d}t}\right)} \quad (4)$$

where T_c is the closure temperature, E_a and D_o are the activation energy and pre-exponential factor for diffusion, respectively, R is the gas constant, a is the effective diffusion radius, $\mathrm{d}T/\mathrm{d}t$ is the cooling rate, and A is a geometric factor. It should be noted, however, that the derivation of this familiar expression rests on several assumptions (Dodson, 1973, 1986); among these is the condition that the diffusant of interest has undergone sufficient exchange with its surroundings such that its initial concentration in the mineral grain is not preserved in any portion of the grain. This assumption, which makes T_c independent of T_o, is, as Ganguly and Tirone (1999) note, not satisfied for slowly diffusing species such as the REEs in garnet and feldspar. Ganguly and Tirone (1999) have developed an extension of Dodson's formalism for closure temperatures taking into consideration systems with arbitrarily small amounts of diffusion.

Fig. 13. Arrhenius plot of REE diffusion in various minerals. REE diffusivities in the feldspars are similar to those for titanite and the middle to heavy REE in cpx. In (a), the three feldspar compositions (solid lines) are plotted with diffusivities for garnet (dotted lines) and clinopyroxene (dashed lines). In (b), diffusivities of Sm and Nd in other minerals are plotted with the plagioclase. Sources for data: diopside—Sm: Sneeringer et al. (1984); Nd, Dy, Yb: Van Orman et al. (2001); orthopyroxene (En_{96})—Ganguly and Tirone (2001); garnet—Nd: Ganguly et al. (1998); Sm: Van Orman et al. (2002); zircon—Cherniak et al. (1997a,b); titanite—Cherniak (1995); YAG—Cherniak (1998a,b); calcite—Cherniak (1998a,b); fluorite—Cherniak et al. (2001); apatite—Cherniak (2000); feldspars—this study.

When the dependence of T_c on T_o is taken into account in calculating closure temperatures, the deviations of these T_c values from closure temperatures calculated using Eq. (4) become smaller with increasing peak temperature (T_o) and slower cooling rate (Ganguly and Tirone, 1999). (For small grain radii, slow cooling rates, and comparatively high peak temperatures, closure temperature curves will converge upon the Dodson values, but significant deviations can exist for larger grains, fast cooling rates and lower peak temperatures.) For example, for Nd diffusion in anorthite, closure temperatures will begin to deviate from Dodson values for grain radii of about 1 mm, given a cooling rate of 10 °C/Ma and peak temperature of 1000 °C; closure temperatures for Nd in oligoclase will begin to depart from values calculated with Dodson's expression for grain radii of one mm with the same cooling rate (10 °C/Ma) and peak temperature of 900 °C.

Further, closure temperatures calculated using Eq. (4) above are mean values, as closure temperature varies with distance from the crystal surface. However, except for a very narrow outermost layer, closure temperatures will not differ from the mean by more than a few tens of degrees for cooling rates between 1 and 10 °C/Ma and grain sizes up to a few mm. It should be clear from the above brief discussion that closure temperature is dependent on many factors. Nonetheless, we can use the Dodson formulation (Eq. (4)) above to make broad comparisons of closure T of REE in various minerals, while recognizing the complexities in determining a "closure temperature" for a given mineral under a given set of geological circumstances. The result of these calculations is shown in Fig. 14. For a cooling rate of 10 °C/Ma and a equal to 1 mm, we obtain closure temperatures for Nd of 890 and 980 °C for oligoclase and anorthite, respectively. Under most geologic circumstances, then, closure temperatures of the REE in feldspar are sufficiently high that grains will not experience significant change in REE composition during a cooling event.

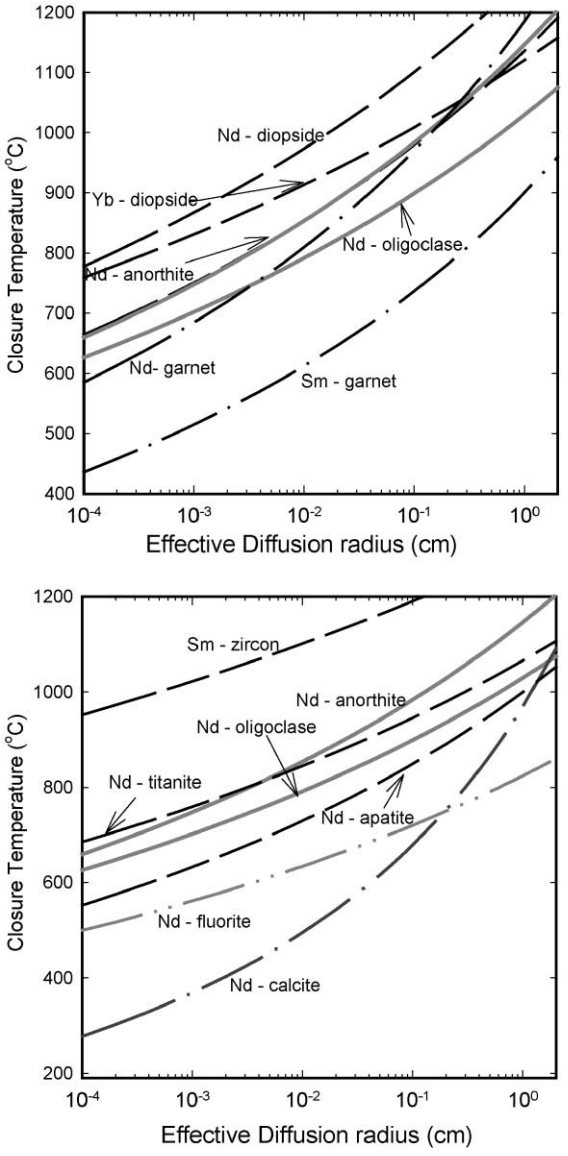

Fig. 14. Closure temperatures for the REE in several minerals as function of effective diffusion radius for a cooling rate of 10 °C per million years. Calculations were made employing the standard expression of Dodson (Eq. (4)). Sources for diffusion data for closure temperature calculations are included in the caption for Fig. 13. Closure temperatures for Sm in diopside and garnet are in a range similar to the REE in feldspar, as is Nd in titanite. However, closure temperatures for Nd (and other LREE) calculated using the diffusion parameters of Van Orman et al. (2001) are significantly higher than those for the feldspars. Closure temperatures for Nd in fluorite and calcite are considerably lower than closure temperatures for feldspar, as are those for apatite, although diffusivities (and thus calculated closure temperatures) do depend on the substitutional mechanism involved in REE exchange in apatite (Cherniak, 2000). Zircon, in contrast, has a much higher closure temperature than the feldspars, with T_c for Sm in excess of 1100 °C even for grain sizes on order of 100 μm.

Acknowledgements

I thank Bruce Watson for helpful advice and discussion during the course of this study. Thanks also to Liz Cottrell for providing a preprint of her work. Thoughtful reviews by James Van Orman and Massimiliano Tirone helped considerably in improving the final version of this manuscript. Thanks to the National Museum of Natural History for providing the labradorite specimen (NMNH #135512-1), and to Don Baker and Don Miller for the other feldspars. This work was supported by grant EAR-9804794 from the National Science Foundation (to E.B. Watson). **[RR]**

References

Anderson, O.L., Stuart, D.A., 1954. Calculation of activation energy of ionic conductivity in silica glasses by classical methods. J. Am. Ceram. Soc. 37, 573–580.

Behrens, H., Johannes, W., Schmalzried, H., 1990. On the mechanisms of cation diffusion processes in ternary feldspars. Phys. Chem. Miner. 17, 62–78.

Bindeman, I.N., Bailey, J.C., 1999. Trace elements in anorthite megacrysts from the Kurile Island Arc: a window to across-arc geochemical variations in magma compositions. Earth Planet. Sci. Lett. 169, 209–226.

Bindeman, I.N., Davis, A.M., Drake, M.J., 1998. Ion microprobe study of plagioclase-basalt partition experiments at natural concentrations of trace elements. Geochim. Cosmochim. Acta 62, 1175–1193.

Blundy, J.D., Wood, B.J., 1991. Crystal-chemical controls on the partitioning of Sr and Ba between plagioclase feldspar, silicate melts, and hydrothermal solutions. Geochim. Cosmochim. Acta 55, 193–210.

Cherniak, D.J., 1995. Diffusion of lead in plagioclase and K-feldspar: an investigation using Rutherford Backscattering and resonant nuclear reaction analysis. Contrib. Mineral. Petrol. 120, 358–371.

Cherniak, D.J., 1996. Strontium diffusion in sanidine and albite, and general comments on Sr diffusion in alkali feldspars. Geochim. Cosmochim. Acta 60, 5037–5043.

Cherniak, D.J., 1998a. REE diffusion in calcite. Earth Planet. Sci. Lett. 160, 273–287.

Cherniak, D.J., 1998b. Rare earth element and gallium diffusion in yttrium aluminum garnet. Phys. Chem. Miner. 26, 156–163.

Cherniak, D.J., 2000. Rare earth element diffusion in apatite. Geochim. Cosmochim. Acta 64, 3871–3885.

Cherniak, D.J., 2002. Ba diffusion in feldspar. Geochim. Cosmochim. Acta 66, 1641–1650.

Cherniak, D.J., Watson, E.B., 1992. A study of strontium diffusion in K-feldspar, Na-K feldspar and anorthite using ion implantation and Rutherford backscattering spectroscopy. Earth Planet. Sci. Lett. 113, 411–425.

Cherniak, D.J., Watson, E.B., 1994. A study of strontium diffusion in plagioclase using Rutherford Backscattering spectroscopy. Geochim. Cosmochim. Acta 58, 5179–5190.

Cherniak, D.J., Hanchar, J.M., Watson, E.B., 1997a. Rare earth diffusion in zircon. Chem. Geol. 134, 289–301.

Cherniak, D.J., Hanchar, J.M., Watson, E.B., 1997b. Tetravalent cation diffusion in zircon. Contrib. Mineral. Petrol. 127, 383–390.

Cherniak, D.J., Zhang, X.Y., Wayne, N.K., Watson, E.B., 2001. Sr, Y and REE diffusion in fluorite. Chem. Geol. 181, 99–111.

Cottrell, E.A., Spiegelman, M., Langmuir, C.H., 2002. Consequences of diffusive reequilibration for the interpretation of melt inlcusions. Geochem. Geophys. Geosyst. 3 (DOI number 10.1029/2001 GC000205).

Crank, J., 1975. The Mathematics of Diffusion, 2nd ed. Oxford University Press.

Dodson, M., 1973. Closure temperature in cooling geochronological and petrological systems. Contrib. Mineral. Petrol. 40, 259–274.

Dodson, M.H., 1986. Closure profiles in cooling systems. Mat. Sci. Forum 7, 145–154.

Ganguly, J., Tirone, M., 1999. Diffusion closure temperature and age of a mineral with arbitrary extent of diffusion: theoretical formulation and applications. Earth Planet. Sci. Lett. 170, 131–140.

Ganguly, J., Tirone, M., 2001. Relationship between cooling rate and cooling age of a mineral: theory and applications to meteorites. Meteorit. Planet. Sci. 36, 167–175.

Ganguly, J., Tirone, M., Hervig, R.L., 1998. Diffusion kinetics of Samarium and Neodymium in garnet, and a method for determining cooling rates of rocks. Science 281, 805–807.

Giletti, B.J., Casserly, J.E.D., 1994. Sr diffusion kinetics in plagioclase feldspars. Geochim. Cosmochim. Acta 58, 3785–3793.

Giletti, B.J., Shanahan, T.M., 1997. Alkali diffusion in plagioclase feldspar. Chem. Geol. 139, 3–20.

Kingsley, J.J., Suresh, K., Patil, K.C., 1990. Combustion synthesis of fine particle rare earth orthoaluminates and yttrium aluminum garnet. J. Solid State Chem. 87, 435–442.

LaTourette, T., Wasserburg, G.J., 1998. Mg diffusion in anorthite: implications for the formation of early solar system planetisimals. Earth Planet. Sci. Lett. 158, 91–108.

Mullen, J.G., 1966. Theory of diffusion in ionic crystals. Phys. Rev. 143, 658–662.

Prinzohofer, A., Papanastassiou, D.A., Wasserburg, G.J., 1992. Samarium–neodymium evolution of meteorites. Geochim. Cosmochim. Acta 56, 797–815.

Reddy, K.P.R., Cooper, A.R., 1982. Oxygen diffusion in sapphire. J. Am. Ceram. Soc. 65, 634–638.

Shannon, R.D., 1976. Revised effective ionic radii and systematic studies of interatomic distances in halides and chalcogenides. Acta Crystallogr., A 32, 751–767.

Shewmon, P., 1989. Diffusion in Solids Minerals, Materials, and Metals Society, Warrendale, PA.

Smith, J.V., Brown, W.L., 1988. Feldspar Minerals. Volume 1:

Crystal Structures, Physical, Chemical and Microstructural Properties, 2nd ed. Springer-Verlag, New York.

Smyth, J.R., Bish, D.L., 1988. Crystal Structures and Cation Sites of the Rock-Forming Minerals. Allen & Unwin, Boston.

Sneeringer, M., Hart, S.R., Shimizu, N., 1984. Strontium and samarium diffusion in diopside. Geochim. Cosmochim. Acta 48, 1589–1608.

Stewart, B., Papanastassiou, D.A., Wasserburg, G.J., 1994. Sm–Nd chronology and petrogenesis in mesosiderites. Geochim. Cosmochim. Acta 58, 3487–3509.

Stewart, B., Papanastassiou, D.A., Wasserburg, G.J., 1996. Sm–Nd systematics of a silicate inclusion in the Caddo IAB iron meteorite. Earth Planet. Sci. Lett. 143, 1–12.

Van Orman, J.A., Grove, T.L., Shimizu, N., 2001. Rare earth element diffusion in diopside: influence of temperature, pressure and ionic radius, and an elastic model for diffusion in silicates. Contrib. Mineral. Petrol. 141, 687–703.

Van Orman, J.A., Grove, T.L., Shimizu, N., Layne, G.D., 2002. Rare-earth element diffusion in a natural pyrope single crystal at 2.8 GPa. Contrib. Mineral. Petrol. 142, 416–424.

Waight, T.E., Maas, R., Nicholls, I.A., 2000. Fingerprinting feldspar phenocrysts using crystal isotopic composition stratigraphy: implications for crystal transfer and magma mingling in S-type granites. Contrib. Mineral. Petrol. 139, 227–239.

Zener, C., 1952. Theory of diffusion. In: Shockley, W., Hollomon, J.H., Maure, R., Seitz, F. (Eds.), Imperfections in Nearly Perfect Crystals. Wiley, New York, pp. 289–314.